

# Quantum Lock-in Force Sensing using Optical Clock Doppler Velocimetry

Ravid Shaniv<sup>1</sup> & Roee Ozeri<sup>1</sup>

March 1, 2016

## Abstract

Force sensors are at the heart of different technologies such as atomic force microscopy or inertial sensing [2, 1, 3]. These sensors often rely on the measurement of the displacement amplitude of mechanical oscillators under applied force. Examples for such mechanical oscillators include micro-fabricated cantilevers [3], carbon nanotubes [4] as well as single trapped ions [5, 6]. The best sensitivity is typically achieved when the force is alternating at the mechanical resonance frequency of the oscillator thus increasing its response by the mechanical quality factor. The measurement of low-frequency forces, that are below resonance, is a more difficult task as the resulting oscillation amplitudes are significantly lower. Here we use a single trapped  $^{88}\text{Sr}^+$  ion as a force sensor. The ion is trapped in a linear harmonic trap, and is electrically driven at a frequency much lower than the trap resonance frequency. To be able to measure the small amplitude of motion we combine two powerful techniques. The force magnitude is determined by the measured periodic Doppler shift of an atomic optical clock transition and the Quantum Lock-in technique is used to coherently accumulate the phases acquired during different force half-cycles. We demonstrate force detection both when the oscillating force is phase-synchronized with the quantum lock-in sequence and when it is asynchronous and report frequency force detection sensitivity as low as  $5.3 \times 10^{-19} \frac{\text{N}}{\sqrt{\text{Hz}}}$ .

Force sensors are important for many applications ranging from computer game consoles to precision measurements of fundamental physics. Most force sensors rely on the displacement of mechanical oscillators as an estimator for the applied force. Trapped atomic ions can be well approximated as harmonic mechanical oscillators that are highly sensitive to electrical forces. Moreover, due to the extremely high quality factor of ion traps, even very small forces that are resonant with the ion-trap harmonic frequency can yield relatively large displacements. The ion displacement amplitude is usually measured through its associated Doppler shift on an optical transition [7]. Previously, ion-trap experiments have demonstrated yocto-Newton range measurement sensitivity [6, 5] of forces that were alternating at frequencies that varied between 50 – 900 kHz. Measuring forces that oscillate at frequencies much lower than this range is a challenge if one wishes to maintain the mechanical resonance condition. This is because as the trap weakens and the resonance

frequency is lowered, the ion departs from the Lamb-Dicke regime which is a pre-condition to many trapped-ions control techniques. Moreover, low trap frequencies result in faster heating times and a loss of sensitivity to displacements. If one wishes to measure forces that oscillate at a frequency of a few hundreds of Hz, for example, there is no alternative but to measure this force when it is off-resonance with mechanical resonance at a much higher frequency, resulting in significantly smaller oscillation amplitude. The measurement of low frequency forces will therefore necessitate high sensitivity Doppler-shift measurement techniques.

The most accurate frequency measurements to date have been performed on narrow optical-clock transitions in laser-cooled atoms or ions. The state-of-the-art frequency comparisons are with fractional uncertainty in the  $10^{-18}$  range [8, 9]. An optical clock transition in a single trapped ion can therefore serve as an excellent mean to measure small Doppler shifts. Previously, periodic Doppler shifts on optical clock transitions, resulting in motional side-bands at the trap harmonic frequency, have been used for precision ion thermometry and sideband cooling. Similarly, motional sidebands can also be used for ion micromotion detection and compensation. The detection of oscillatory motion through its associated periodic phase modulation is ultimately limited by the transition phase noise at the relevant frequency. Since optical atomic clocks with transition linewidths narrower than one Hz have been demonstrated, forces that are oscillating in the 10 - 1000 Hz range can be readily detected.

Sideband spectroscopy is a very useful measurement technique. However, when the phase modulation amplitude is small the sideband decreases linearly with the modulation depth. Moreover, the small sideband is often difficult to differentiate from the noisy background. An efficient method of measuring an oscillating signal by a quantum probe, in the presence of noise, is the Quantum lock-in technique [10]. Here, a probe superposition is time modulated by a Hamiltonian term, e.g.  $\hat{\sigma}_x$ , that does not commute with the noise and signal operators, e.g.  $\hat{\sigma}_z$ . The resulting dynamics decouples the probe phase evolution from any frequency component that does not spectrally overlap with the probe modulation and enables a significant prolongation of the probe coherence. On the other hand, frequency components that match some part of the modulation spectrum yield a phase which accumulates as the probe evolves with time. If the desired signal spectrally overlaps with the probe modulation it imprints a coherently-accumulated phase signal which can be subsequently measured. Quantum lock-in detection of different probes has recently led to high-precision magnetometry as well as electric field measurements [12, 13, 11]. In a recent experiment this technique was also used in order to evaluate the phase-noise spectral density of an optical atomic clock [14].

Here we use an optical atomic clock transition in a single trapped  $^{88}\text{Sr}^+$  ion and the quantum lock-in technique for the purpose of force metrology. The ion is trapped in a linear Paul trap with radial frequencies close to 2.3 MHz, and axial frequency of 1.13 MHz, and Doppler cooled to a temperature of  $T = 2 \text{ mK}$  on a strong dipole allowed transition at 422 nm. The optical clock transition we use for force measurement is the  $S_{1/2} \rightarrow D_{5/2}$  electric quadrupole transition at a wavelength of 674 nm and a natural linewidth of approximately 0.4 Hz. The clock laser beam crosses the trap axis, and therefore the direction of ion motion at an angle of  $45^\circ$ . At our temperature the resulting Lamb-Dicke parameter for this transition,  $\eta = 0.06$ ,

is sufficiently small to allow for resolved motional sidebands to be observed and a Doppler-free Carrier transition. Detection of successful electron-shelving to the  $D_{5/2}$  level is performed through state selective fluorescence on the 422nm transition. The meta-stable  $D$  levels are depleted using two infra-red re-pump lasers. A schematic diagram of the atomic levels involved is shown in Fig. 1b. More details about our experimental set-up can be found in [15]

Our clock laser is based on an external-cavity diode laser that is pre-stabilized to a high-finesse ( $f = 100,000$ ) cavity made of Ultra-Low Expansion (ULE) glass. To filter out high frequency phase noise we use the cavity as a narrow optical transmission filter. The light transmitted through this cavity is injected into a bare slave diode laser [16]. This injected diode laser is further stabilized to another high-finesse ( $f = 300,000$ ) ULE glass cavity. The resulting laser line-width at a time of 100 seconds is below 100 Hz. Slow drifts ( $0.1 \text{ Hz/sec}$ ) in the cavity resonance frequency are mitigated by periodic calibration of the laser frequency to the optical clock transition. The two, optically-separated, levels used for force detection are  $(5S_{\frac{1}{2}}, m_{\frac{1}{2}} = -\frac{1}{2})$  and  $(4D_{\frac{5}{2}}, m_{\frac{5}{2}} = \frac{1}{2})$ , hereafter denoted as  $|S, \frac{1}{2}\rangle$  and  $|D, -\frac{1}{2}\rangle$  respectively.

Under a constant-amplitude driving force which is far from resonance, the ion harmonic oscillator steady-state motion is given by,

$$x(t) = x_0 \cos(2\pi f_m t) = \frac{F_0}{4\pi^2 (f_t^2 - f_m^2) m_{ion}} \cos(2\pi f_m t). \quad (1)$$

Here,  $F_0$  is the force amplitude,  $m_{ion} = 87.9 \text{ amu}$  is the ion mass,  $f_m = 1.013 \text{ kHz}$  and  $f_t = 1.13 \text{ MHz}$  are the force driving frequency and trap harmonic frequency respectively. The amplitude of the ion motion is linearly proportional to the amplitude of the driving force with a linear coefficient  $(4\pi^2 (f_m^2 - f_t^2) m_{ion})^{-1}$ . With all above parameters pre-determined,  $F_0$  can be estimated from a measurement of the ion motion amplitude.

The amplitude of motion is determined by a measurement of the associated Doppler shifts of the clock transition using Ramsey spectroscopy. Initializing the ion in the an equal superposition of the clock states, it will evolve in time as,

$$\psi(t) = \frac{1}{\sqrt{2}} \left( \left| S, \frac{1}{2} \right\rangle + e^{i\phi_{clk}(t)} \left| D, -\frac{1}{2} \right\rangle \right), \quad (2)$$

where  $\phi_{clk}(t) = \int_0^t \delta(\tau') d\tau'$  and  $\delta(\tau)$  is the frequency difference between the resonance frequency of the ion transition in its rest frame and the laser frequency at time  $\tau$ . The periodically driven ion motion results in a periodic Doppler shift and therefore,

$$\phi_{clk}(t) = \frac{2\pi x_0}{\sqrt{2}\lambda} [\sin(2\pi f_m t + \xi) - \sin(\xi)]. \quad (3)$$

Here,  $\lambda$  is the laser wavelength and  $\xi$  is the phase of the driving force at the beginning of the Ramsey sequence.

Since the clock superposition phase is periodically oscillating, for  $\xi = 0$  it is maximal at quarter of the

force cycle but will have a zero average at longer times. Moreover, optical phase noise will lead to dephasing of the optical clock and loss of phase information. In order to accumulate the Doppler-shift phase over multiple force cycles and prolong the clock coherence we used the quantum lock-in method [13]. To this end, a train of optical echo pulses modulated the clock superposition. Each block in the modulation sequence is composed of a wait time  $\tau$  followed by a  $\pi$ -pulse on the optical clock transition and another equal wait time  $\tau$ . This block is repeated  $n$  times. Using this sequence the superposition phase is modulated during the Ramsey sequence;  $\phi_{clk}(t) = \int_0^t \delta(\tau', \xi) F_{mod}(\tau', \tau, n) d\tau'$ ; where the modulation function,

$$\Pi\left(\frac{t}{2n\tau}\right) \left[ \Theta(t) + 2 \sum_{k=1}^{\infty} (-1)^k \Theta(t - (2k-1)\tau) \right], \quad (4)$$

is a square wave modulation, where  $\Pi\left(\frac{t}{2n\tau}\right)$  is a rectangular function which nulls outside the range  $|t| < \tau n$  where it is equal unity and  $\Theta(t)$  is the Heaviside step function. An example modulation for  $n = 4$  is plotted in Fig. 1a. Modulating the phase improves on the measurement signal-to-noise-ratio in two ways. First, by choosing  $\tau$  and  $\xi$  correctly, e.g.,  $\tau = \frac{1}{4f_m}$  and  $\xi = 0$ , the phase of the superposition accumulates over multiple force cycles rather than oscillating around a zero mean. For the above choice the phase evolution will be  $\phi_{clk}(t) = \frac{4\pi^2}{\sqrt{2}\lambda} f_m x_0 \int_0^t |\cos(2\pi f_m \tau')| d\tau'$ . In addition, this modulation dynamically decouples the ion from noise components at frequencies other than harmonic multiples of  $\frac{1}{4\tau}$  [10]. It should be noted that other modulation sequences can be chosen as well, as long as they have a good spectral overlap with the force frequency. Here we use a train of echo pulses, which result in a square wave phase modulation, due to its implementation simplicity and short exposure of the superposition states to light.

The experiment sequence was as follows. The ion was constantly driven by an oscillating force resulting in periodic motion as in Eq. (1). Its electronic state was initialized to  $|S, -\frac{1}{2}\rangle$ , using optical pumping to  $|S, \frac{1}{2}\rangle$  followed by a radio-frequency  $\pi$  pulse. After initialization, a clock laser  $\frac{\pi}{2}$  pulse initialized the equal superposition of clock state in Eq. (2). This pulse was timed by an external trigger at a constant phase of the driving force to determine  $\xi$ . Subsequently, the modulation sequence of  $n$  echo pulses described above, with  $\tau = \frac{1}{2}f_{mod}$ , was executed. The sequence concluded with a second clock laser  $\frac{\pi}{2}$  pulse, with laser phase  $\phi$  relative to the initial  $\frac{\pi}{2}$  pulse phase. Following the Ramsey experiment the ion state was detected using state-selective fluorescence.

Figure 2a shows the probability of finding the ion in the  $D$  level after the Quantum lock-in sequence as a function of the second  $\frac{\pi}{2}$  pulse phase,  $\phi$ . The superposition phase,  $\phi_{clk}$ , was estimated by a maximum likelihood fit of our data to  $f(\phi) = \frac{1}{2} + \frac{C}{2} \cos(\phi - \phi_{clk})$ , where  $C$  accounts for fringe contrast reduction due to dephasing. Such a reduction in contrast will compromise the phase estimation accuracy. To extract the modulating force from the  $\phi_{clk}$ ,  $\xi$  and  $f_m$  have to be precisely known. To avoid systematic uncertainties in these two parameters we scanned both  $\tau$  and  $\xi$  and measured  $\phi_{clk}$  for every value. The expected  $\phi_{clk}$  for every  $\tau$  and  $\xi$  can be analytically calculated to be,

$$\phi_{clk} = \frac{4\pi x_0}{\sqrt{2}\lambda} \frac{\cos(2\pi f n \tau + \xi + n\frac{\pi}{2})}{\cos(2\pi f \tau)} \sin\left(2\pi f n \tau - n\frac{\pi}{2}\right) \sin^2(\pi f \tau). \quad (5)$$

The theoretically calculated  $\phi_{clk}$  vs.  $\tau$  and  $\xi$  and our experimental results are shown in Figures 2b and 2c respectively, for a lock-in sequence with  $n = 10$  and  $f_m = 1013 \text{ Hz}$ . As seen, our results are in good agreement with the theoretical predictions. We estimated the motion amplitude of the ion to be  $x_0 = 117.5 \pm 0.5 \text{ nm}$ , by a maximum likelihood fit of Eq. 5 to the data. Since no significant reduction of contrast was observed, the uncertainty in our measurement was dominated by quantum projection noise. Using Eq. 1 we inferred a force magnitude of  $F_0 = 8.64 \pm 0.03 \times 10^{-19} \text{ N}$ . With a total experiment time of roughly 9 Hours, our force estimation sensitivity is  $5.3 \times 10^{-19} \frac{\text{N}}{\sqrt{\text{Hz}}}$ .

Thus far we treated the case in which the frequency and the phase of force exerted on the ion are coherently locked with respect to the lock-in sequence. However, in many cases, the phase of the force is unknown, and perhaps also changes with time. In the case where there is a continuous force spectrum, decoherence spectroscopy can be used in the limit of a Gaussian distributed or sufficiently weak force which imparts small ( $\ll 2\pi$ ) phases on the clock superposition to estimate the force spectral density [17, 18, 19]. In cases where the force spectrum is composed of discrete tones, the clock superposition can be used as force frequency and amplitude detector with sub-Fourier frequency estimation [10]. To demonstrate such incoherent force estimation, we repeated our measurements without triggering the quantum lock-in sequence at a constant force phase. Since the experiment is repeated at a rate which is incommensurate with the force frequency, the phase  $\xi$  is sampled with uniformed probability in different repetitions of the experiment. After averaging over all possible  $\xi$  the quantum lock-in fringe contrast can be shown to be given by [10],

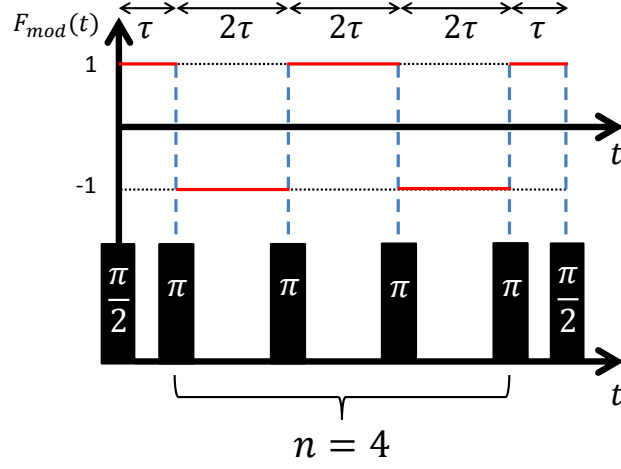
$$C(\tau, n) = \frac{1}{2} + \frac{1}{2} J_0 \left( \frac{4\pi x_0}{\sqrt{2}\lambda} \frac{\sin(2\pi f n \tau - n\frac{\pi}{2}) \sin^2(\pi f \tau)}{\cos(2\pi f \tau)} \right), \quad (6)$$

where  $J_0$  is the zero-order Bessel function of the first kind. The contrast,  $C(\tau, n)$  is estimated by maximum likelihood fits to quantum lock-in phase scans as ion the coherent force detection case. Four example fringes are shown in Fig. 3a showing the effect of noise with the same force amplitude, but different  $\tau$  values. As seen, initially  $C(\tau, n)$  decreases with increased  $\tau$ , resulting in larger phase variance due to the random Doppler shift, until when the phase variance approaches  $\pi/2$  the fringe contrast nearly vanishes. However, as  $\tau$  is further increased the fringe contrast re-appears with a  $\pi$  phase shift (negative  $C(\tau, n)$ ). This is due to the fact that when the phase variance approaches  $\pi$  the different realizations partially re-phase and overlap. The measured contrast,  $C(\tau, n)$ , for an un-synchronized force detection is shown in Fig. 3b, 3c for  $n = 10, 20$  respectively. The endcap modulation was similar to the synchronized experiment - amplitude of 30 mV and frequency of  $f_m = 1013 \text{ Hz}$ . Each contrast measurement was performed twice - with and without a driving force. The measured contrast was taken to be the ratio between the two measurements, in order to reject contrast decrease due to un-related effects, such as laser phase noise or  $D$  level spontaneous decay. The solid line is a maximum likelihood fit of Eq. 6 to our data. We used two fit parameters, the motion amplitude

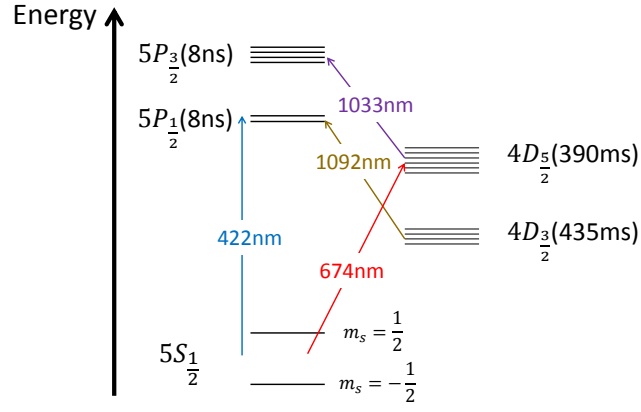
$x_0$  and the modulation frequency  $f_m$ . As seen, the theoretical prediction of Eq. 6 and our measured data are in good agreement. The frequency we measure is  $f_m = 1015 \pm 2 \text{ Hz}$ . In both cases, the fitted value for  $f_m$  was within a 4 Hz wide 95% confidence interval around the actual value. As mentioned above, with this method the frequency of the force can be estimated with sub-Fourier uncertainty [10], that results from the non-linear response of the ion to the force drive that generates the narrow features appearing in Fig. 3b, 3c. The motion amplitude was estimated by the fit to be  $x_0 = 116 \pm 3 \text{ nm}$  and  $x_0 = 115 \pm 4 \text{ nm}$ , corresponding to  $F_0 = 8.54 \pm 0.2 \times 10^{-19} \text{ N}$  and  $F_0 = 8.47 \pm 0.3 \times 10^{-19} \text{ N}$  for  $n = 10, 20$  pulses respectively. The measurement sensitivity for  $n = 10, 20$  was  $1.7 \times 10^{-18} \frac{\text{N}}{\sqrt{\text{Hz}}}$  and  $2 \times 10^{-18} \frac{\text{N}}{\sqrt{\text{Hz}}}$  respectively. This result agrees with the force amplitude estimated in the case when the force phase was known.

To conclude, we demonstrated an oscillating-force detection method using a single trapped ion. Our method uses an optical clock superposition phase as a measure of the ion amplitude of motion. We used a quantum lock-in technic in order to amplify the desired signal while reducing the effect of unwanted spectral components with dynamic decoupling. This technique allows us to measure forces at low frequencies, much lower than the trapping frequency. We demonstrated different methods for the case in which the phase of the oscillating force is known and for the case when it is unknown, and we got sensitivity of  $5.3 \times 10^{-19} \frac{\text{N}}{\sqrt{\text{Hz}}}$ . This sort of measurement can be useful for sensitive detection of electric fields close to a surface.

During the writing stages of this manuscript we become aware of a similar theoretical proposal for force sensing [20]. This work was supported by the Crown Photonics Center, ICore-Israeli excellence center circle of light, the Israeli Science Foundation, the Israeli Ministry of Science Technology and Space, and the European Research Council (consolidator grant 616919-Ionology)

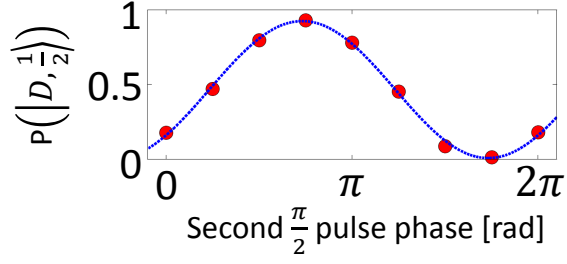


(a)

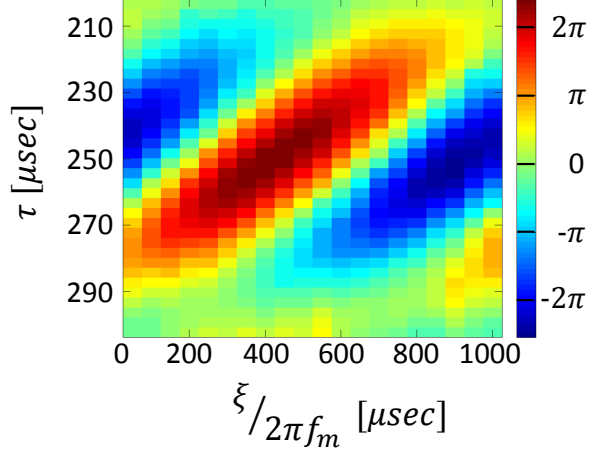


(b)

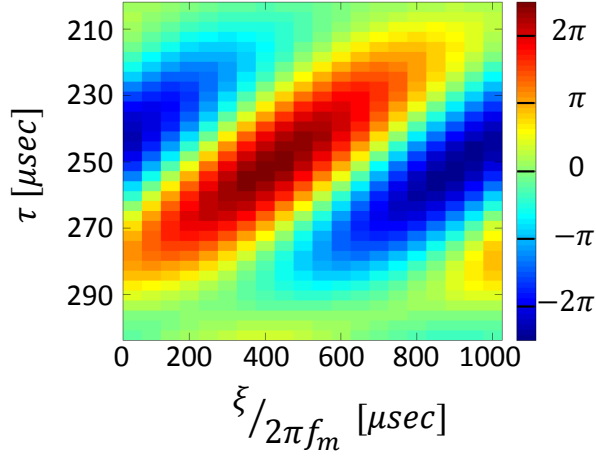
Figure 1: **(a)** Modulation function  $F_{mod}(t, \tau, n=4)$  (upper timeline) and the corresponding experimental pulse sequence (lower timeline). **(b)**  $^{88}\text{Sr}^+$  ion relevant level scheme, levels lifetime and laser wavelengths.



(a)



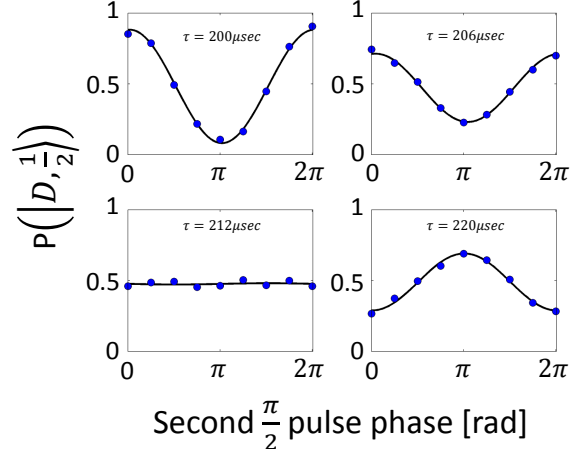
(b)



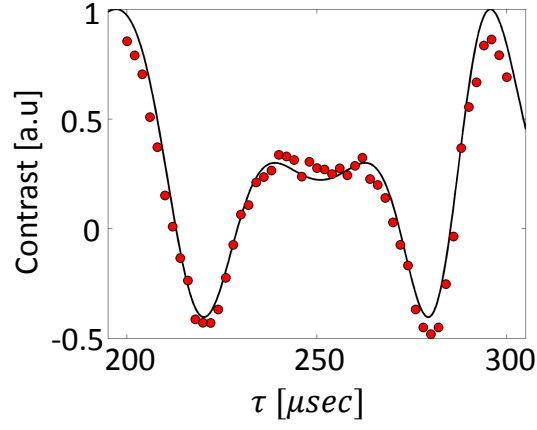
(c)

Figure 2: Experimental results of quantum lock-in force measurement. **(a)** A typical Ramsey fringe from which the superposition phase is estimated. **(b)** Measured Phase as a function of  $\tau$  and  $\xi$ . Each point on the plot corresponds to the phase extracted from a measurement similar to (a). The phase offset  $\xi$  is affected by different technical delays in our system. **(c)** Theoretical calculation for (b) using Eq. 5 with  $A = \frac{2\pi x_0}{\sqrt{2}\lambda}$  and  $\xi$  as fitted from (b). The calculated value for the phase amplitude is  $A = 0.774 \pm 0.004$  rad, corresponding to  $x_0 = 117.5 \pm 0.5$  nm and  $F_0 = 8.64 \pm 0.03 \times 10^{-19}$  N.

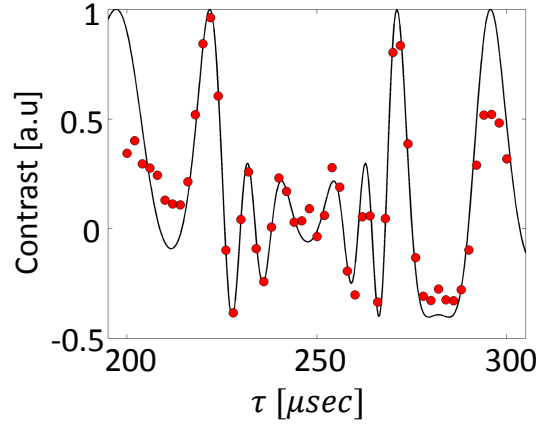




(a)



(b)



(c)

Figure 3: Experiment results of a-synchronous force measurement. **(a)** Four different contrast fringes measured at different modulation frequencies for  $n = 10$  echo pulses. As the ion modulation frequency approaches the force modulation frequency (1013 Hz) the phase variance increases and the fringe contrast decays. The last fringe (1136 Hz) shows partial re-phasing due to the topology of the Bloch sphere. **(b),(c)** Measured contrast as a function of  $\tau$  with  $n = 10, 20$  echo pulses correspondingly. Each point on the plot corresponds to the contrast extracted from a measurement similar to (a). The fit correspond to Eq. 6. The calculated value for the ion motion amplitudes  $q_s$   $x_0 = 116 \pm 3$  nm and  $x_0 = 115 \pm 4$  nm, and the corresponding force amplitudes are  $F_0 = 8.54 \pm 0.2 \times 10^{-19}$  N and  $F_0 = 8.47 \pm 0.3 \times 10^{-19}$  N for  $n = 10, 20$  pulses respectively.

## References

- [1] Rugar, D., Budakian, R., Mamin, H. J. & Chui B. W. Single spin detection by magnetic resonance force microscopy. *Nature* 430, 329-332 (2004).
- [2] Giessibl, F. J. Advances in atomic force microscopy. *Rev. Mod. Phys.* 75, 949 (2003).
- [3] Yazdi, N., Ayazi, F., & Najafi, K. Micromachined Inertial Sensors. *proceedings of the IEEE*, 86, pp. 1640-1659, (1998)
- [4] Moser, J., Güttinger, J., Eichler, A., Esplandiu, M. J., Liu, D. E., Dykman, M. I. & Bachtold, A. Ultrasensitive force detection with a nanotube mechanical resonator. *Nature Nanotechnology* 8, 493-496 (2013).
- [5] Biercuk, M. J., Uys, H., Britton, J. W., VanDevender, A. P. & Bollinger, J. J. Ultrasensitive detection of force and displacement using trapped ions. *Nature Nanotechnology* 5, 646-650 (2010).
- [6] Knünz, S., Hermann, M., Batteiger, V., Saathoff, G., Hänsch, T. W., Hala, K. & Udem, Th. Injection locking of a trapped-ion phonon laser. *Phys. Rev. Lett.* 105, 013004 (2010).
- [7] Liebfried, D., Blatt, R., Monroe, C. & Wineland, D. Quantum dynamics of single trapped ions. *Rev. Mod. Phys.* 75, 281 (2003).
- [8] Chou, C. W., Hume, D. B., Koelemeij, J. C. J., Wineland, D. J. & Rosenband, T. Frequency Comparison of Two High-Accuracy  $\text{Al}^+$  Optical Clocks. *Phys. Rev. Lett.* 104, 070802 (2010).
- [9] Bloom, B. J., Nicholson, T. L., Williams, J. R., Campbell, S. L., Bishof, M., Zhang, X., Zhang, W., Bromley, S. L. & Ye, J. An optical lattice clock with accuracy and stability at the  $10^{-18}$  level. *Nature*, 506, 71-75, (2014).
- [10] Kotler, S., Akerman, N., Glickman, Y. & Ozeri, R. Nonlinear single-spin spectrum analyzer. *Phys. Rev. Lett.* 110, 110503 (2013).
- [11] Staudacher, T., Shi, F., Pezzagna, S., Meijer, J., Du, J., Meriles, C. A., Reinhard, F. & Wrachtrup, J. Nuclear Magnetic Resonance Spectroscopy on a (5-Nanometer) Sample Volume. *Science*, 339, 6119, pp. 561-563 (2013).
- [12] Taylor, J. M., Cappellaro, P., Childress, L., Jiang, L., Budkers, D., Hemmer, P. R., Yacobi, A., Walsworth, R., & Lukin, M. D. High-sensitivity diamond magnetometer with nanoscale resolution. *Nature Physics* 4, 810 - 816 (2008).
- [13] Kotler, S., Akerman, N., Glickman, Y., Keselman, A. & Ozeri, R. Single-ion quantum lock-in amplifier. *Nature* 473, 6165 (2011).

- [14] Bishof, Michael, et al. "Optical spectrum analyzer with quantum-limited noise floor." *Phys. Rev. Lett.* 111.9 (2013): 093604.
- [15] Akerman, N., Glickman, Y., Kotler, S., Keselman, A. & Ozeri, R. Quantum control of  $88\text{Sr}^+$  in a miniature linear Paul trap. *Applied Physics B* 107, 1167-1174 (2012).
- [16] Akerman, N., Navon, N., Kotler, S., Glickman, Y. & Ozeri, R. Universal gate-set for trapped-ion qubits using a narrow linewidth diode laser. *New J. Phys.* 17 (2015).
- [17] Lasič, S., Stepišnik, J., & Mohorič, A. Displacement power spectrum measurement by CPMG in constant gradient. *Journal of Magnetic Resonance*, 182, 208214 (2006).
- [18] Cywiński, L., . Lutchyn, R. M., Nave, C. P. & . Das Sarma, S. How to enhance dephasing time in superconducting qubits. *Phys. Rev. B.* 77, 174509 (2008).
- [19] Hall, L. T., Cole, J. H., Hill, C. D. & Hollenberg, L. C. L. Sensing of Fluctuating Nanoscale Magnetic Fields Using Nitrogen-Vacancy Centers in Diamond. *Phys. Rev. Lett.* 103, 220802 (2009).
- [20] Ivanov, P. A., Vitanov, N. V. & Singer K. High-precision force sensing using a single trapped ion. <http://arxiv.org>, 1602.04072 (2016).